WILEY-VCH

Hereditary character of photonics structure in *Pachyrhynchus sarcitis* weevils: color changes *via* one generation hybridization

Yin Chang, Yu Ogawa, Gianni Jacucci, Olimpia D. Onelli, Hui-Yun Tseng*, Silvia Vignolini*

Yin Chang. Author 1, Gianni Jacucci. Author 3, Dr. Olimpia D. Onelli. Author 4, Dr. Silvia Vignolini. Author 6

Department of Chemistry, University of Cambridge, Cambridge CB2 1EW, United Kingdom
E-mails: hytseng1216@gmail.com ; sv319@cam.ac.uk

Dr. Yu Ogawa. Author 2
University Grenoble Alpes, CNRS, Cermav, 38400, France.

Dr. Hui-Yun Tseng. Author 5
Department of Entomology, National Taiwan University, 106, Taiwan.

Abstract

Pachyrhynchus sarcitis weevils are flightless weevils characterized by colored patches of scales on their dark elytra. The vivid colors of such patches result from the reflection of differently oriented three-dimensional photonic crystals within their scales. Our results show that hybrid *P. sarcitis*, the first filial generation of two *P. sarcitis* populations from Lanyu Island (Taiwan) and Babuyan Island (Philippines), mixes the color of its ancestors by tuning the photonic structure in its scales. A careful spectroscopical and anatomical analysis of the weevils in the phylogeny reveals the hereditary characteristics of the photonic crystals within their scales in terms of lattice constant, orientation and domain size. Monitoring how structural coloration is inherited by offspring highlights the versatility of photonic structures to completely redesign the optical response of living organisms. Such finding shed light onto the evolution and development mechanisms of structural coloration in *Pachyrhynchus* weevils and provides inspiration for the design of visual appearance in artificial photonic materials.

1

1. Introduction

Structural colors, i.e. colors originating from interactions of light and nano-structured materials, are incredibly widespread in living organisms. [1–3] From bacteria, [4] to plants, [5,6] insects, [7–13] and larger animals. [14–16] Different organisms produce bright colorations with various mechanisms and for diverse functions. [3,6,16–19] Within the wide variety of architectures and materials exploited by different organisms, insects produce exquisitely complex three-dimensional photonic architectures. [17,20–22] In the Curculionidae weevil family, most of the species have three-dimensional diamond photonic crystal structures and many species exploit diamond photonic crystals with different volume fractions [22,23] and lattice constants [22,23,28] to obtain a wide variety of colorations.

Pachyrhynchus weevils possess a dark exoskeleton marked with colorful patterns. As they are flightless, they are distributed exclusively on several islets of Southeast Asia, and display high insular species diversity. [29,30] So far, their taxonomy is based only on their optical appearance [31–33] and this poor understanding of their ecology often leads to species misidentification. [34] Moreover, some pioneering works reported incorrect crystal structures [35,36] and only recent studies [20,22,27] correctly analyzed the morphology and the optical response of the weevils' scales.

While the optical properties of *Pachyrhynchus* weevils are well characterised and already fascinated several groups in the field, the understanding on how the structural color phenotype is inherited by hybrid weevils, and more in general for insects, is still missing, as it is challenging to grow these species in captivity. [37]

In this work, we optically and anatomically monitor the evolution of the diamond photonic structure of *P. sarcitis via* a hybridization technique. In particular, we observe that, irrespectively of the sex of the parents, the first-generation cross between captive-bred blue-

2

spotted (Lanyu Is., Taiwan) and yellow-spotted *P. sarcitis* weevils (Babuyan Is., Philippines) inherits a green structural coloration. Such green coloration is not the result of a diamond structure with intermediate lattice constant or chitin filling fraction of the parent weevils, but is related to the orientations and size of the different crystal domains within their scales.

By combining the statistical information on the morphology of the crystal, domain sizes, and orientations (obtained by multi-directional scanning electron microscope (SEM) images) with the numerical calculation, we reproduce the measured optical response. Our results reveal the significance of the preferred domain orientations on the visual appearance of the weevil scales, providing important insights on the factors shaping the evolution of structural colors in weevils. In fact, the tuning of the distribution of the domain orientations might be a convenient strategy to achieve different colorations, strengthening the hypothesis of the self-assembly characteristics of the morphogenesis of photonic structures in insects *via* phase separation processes. [7,17,21] Finally, we discuss how these findings might provide a convenient strategy to optimise visual appearance with structurally colored materials.

2. Results

### 2.1. Optical appearance and reflection spectra of weevils' scales

All three *P. sarcitis* weevils exhibit patterns of colored patches of scales in similar locations on their dark exoskeletons (**Figure 1**). Macroscopically, the Lanyu *P. sarcitis* (LPS) has blue and cyan scales (Figure 1 A), Babuyan *P. sarcitis* (BPS) has predominantly green and yellow scales (Figure 1 B), while their offspring, hybrid *P. sarcitis* (HPS), has green scales (Figure 1 C).
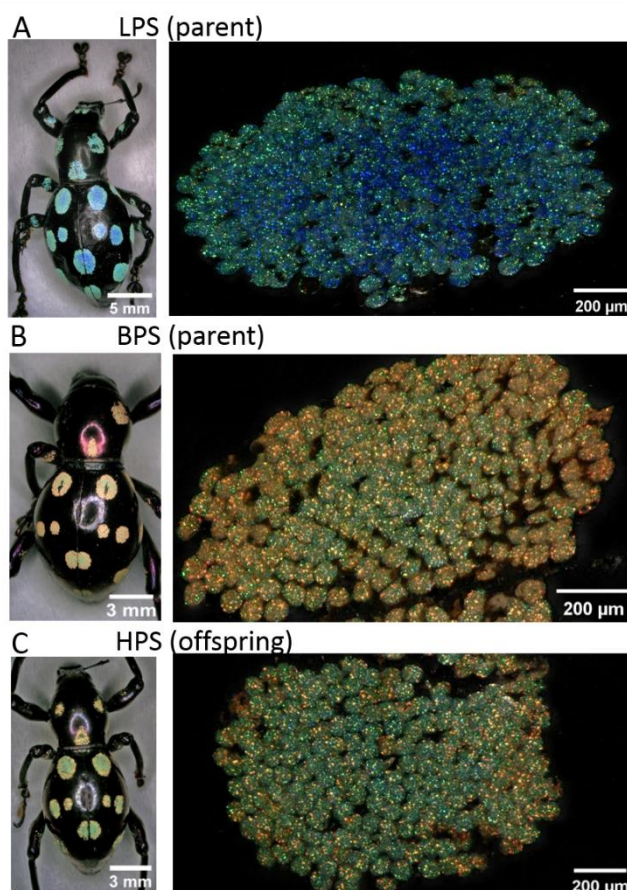
Figure 1 Three *Pachyrhynchus sarcitis* (*P. sarcitis*) used in this study and the enlarged image of a single pit of each weevil. (**A**) Lanyu *P. sarcitis* (LPS, from Lanyu Is., Taiwan) and (**B**) Babuyan *P. sarcitis* (BPS, from Babuyan Is., Philippines) are captive species. (**C**) Hybrid *P. sarcitis* (HPS) is the filial generation of LPS and BPS. For all three weevils each pit is covered by many small scales.

In the epi-illumination microscope pictures reported in **Figure 2** A- C, we can observe that for all three weevils every scale shows differently colored areas (domains) with colors in the entire visible spectral range. Therefore, in order to quantitatively correlate how such domains cumulatively contribute to the overall optical appearance, we measured: (i) the reflection spectrum of each single domain in several areas for all three weevils (in terms of spectral position and intensity), (ii) their lateral size, and (iii) their abundance. Representative spectra are reported in Figure 2 D- F, while all spectra, images, domain color histograms, and their

statistic domain color coverage for the examined scales are provided in Supporting

Information Figure S1, S2 and Table S1.
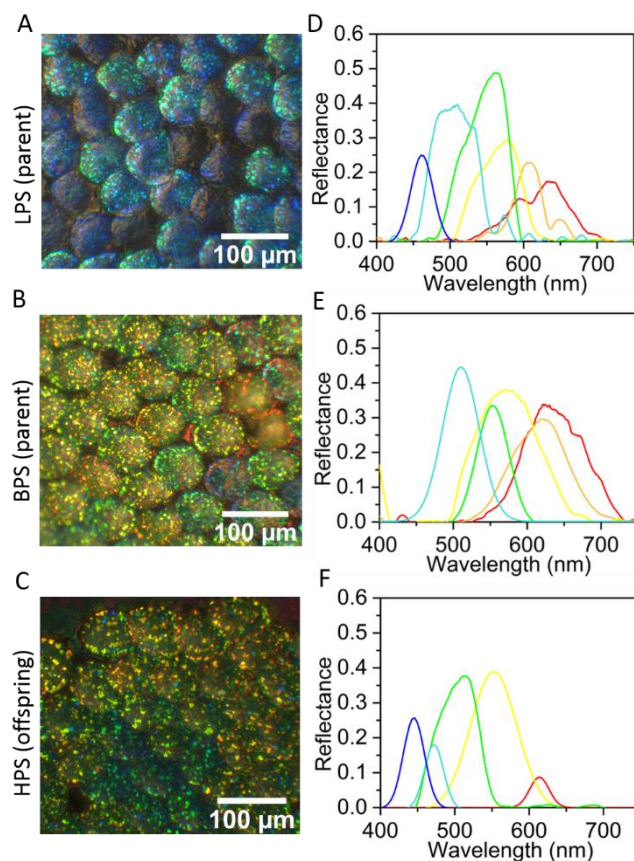
Figure 2 Differently colored domains within scales and representative reflected spectra of

each domain color in three weevils. (**A-C**) Domains with different colors can be recognized in

each scale of all three weevils. Blue, yellow, and green are dominate color in LPS, BPS, and

HPS, respectively. (**D-F**) The representative spectra for LPS, BPS and HPS originating from

differently colored domains in the scales.

As reported in Figure 2, for all three weevils it is possible to find domains reflecting colors

across the entire visible spectral range from blue to red, with a full width at half maximum

(FWHM) of ranging from 30 to 108 nm, with generally, a larger FWHM for red-shifted

peaks. Interestingly, we notice that the intensity of the reflection peaks varies in different

weevils depending on the spectral region: as an example, cyan and green are the most

intensely reflected colors in LPS. While, in BPS, all the reflected colors have a comparable

reflectance, and the HPS exhibits a higher reflectance of green and yellow.

2.2. Domain orientations and lattice parameters

To quantify the size and occurrence of the domains, we imaged the photonic crystal structures

inside the scales *via* SEM both from above and in cross-section (see **Figure 3**); detailed

sample preparation is described in Experimental Section. Multiple crystal orientations were

observed from both top views (Figure 3 B, C, D) and cross-sectional views (Figure 3 E- G),

indicating that crystals rotate in three dimensions in all three weevils. The typical patterns of

the diamond crystal orientations (100), (110), (111) have been observed in all three weevils

(Figure 3. A- D). From SEM images of (111), we estimated the lattice constant, a, while we

measured the strut radius, b, from cross-sectional SEM images of (110) orientation, as, in this

direction, the strut is perpendicular to the observation plane. The air pore radius, R, is then

calculated from the measured strut radius and lattice constant with the diamond lattice

structure relation: $R = {}^a\!/_2 - \sqrt{2}b$, see also Figure S3 and Table S2 and the Supporting

Information for additional details.
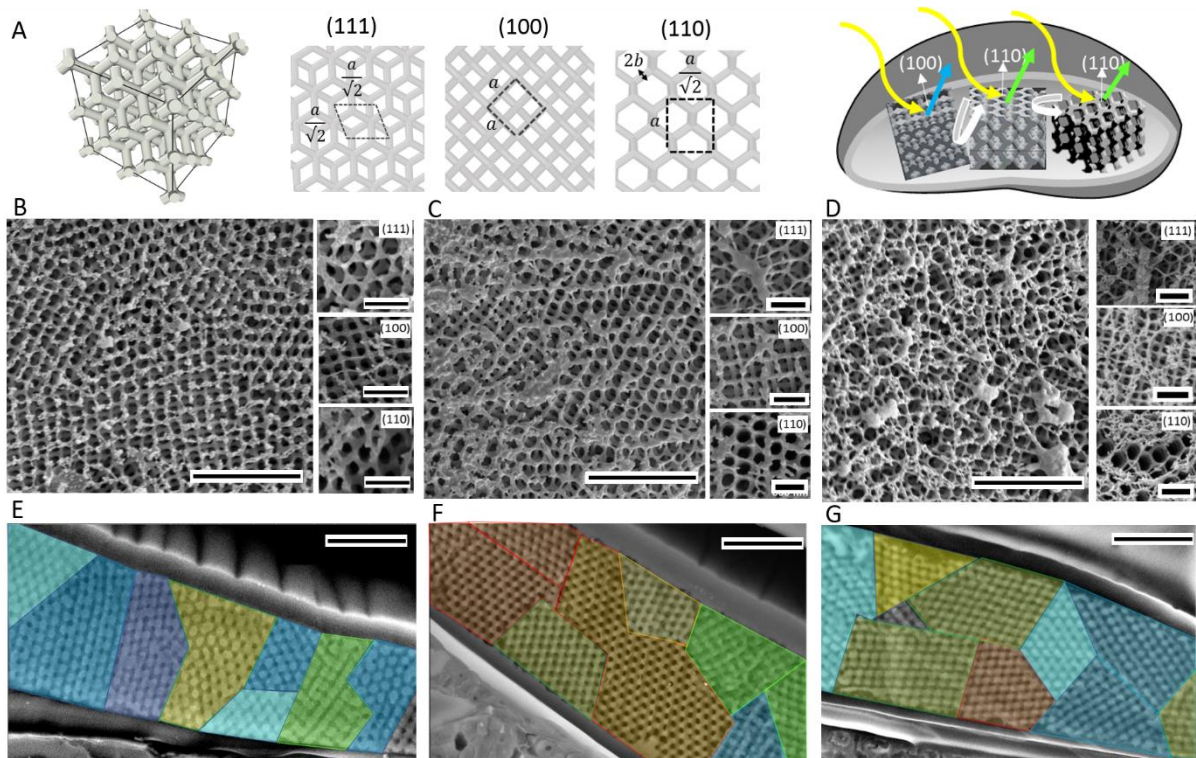
Figure 3 Three-dimensional photonic crystals with single diamond lattice structure (Fd-3m) in three weevils and mapping domain orientations and reflected color normal to the scale surfaces. (**A**) Illustrations of a single diamond lattice and its three characteristic orientations: (111), (100), (110). Lattice constant,a, can be calculated from the three characteristic orientations. Different oriented domains rotating horizontally (azimuth angle φ) or tilting (polar angle θ) from crystal normal [100] are observed in both top view and cross-section SEM images in (**B, E**) LPS, (**C, F**) BPS, and (**D, G**) HPS confirm that different color domain correspond to different crystals orientations for three weevils. Scale bars in (**B- G**) are 2 μm, while in (111), (100), (110) images are 500 nm. It is possible to observe in three weevils, at the side of one scale, top and base of the shell is connected by one domain as shown in (**B**) LPS, or by two domains as in (**C**) BPS (**D**) HPS.

Quantitative structural information was obtained by sampling over a large number of regions within scales and between scales from different areas of the weevils' exoskeleton. The average

strut radius, lattice constant, pore radius and filling fraction (FF of diamond minimum surface

model) for the three weevils are shown in **Table 1**. It is interesting to highlight that all three

weevils have similar strut radii of 57-59 nm and FF of 0.4. In contrast, the LPS weevil has a

lattice constant of $a = 413 \pm 5\ nm$, while BPS and HPS have similar values for the lattice

constant ($a = 439 \pm 7\ nm$ and $a = 444 \pm 5\ nm$, respectively).

Table 1. Measured strut radius and lattice constant from SEM images, and the calculated pore

radius and filling fraction of the three weevils.

	LPS (parent)	BPS (parent)	HPS (offspring)
Strut radius, r (nm)	58.5± 6.5	57.4± 5.9	59.4± 6.2
Lattice constant, a (nm)	412.8± 5.4	438.5± 6.7	443.9± 5.4
Pore radius (calculated)	123.7± 9.6	138.1± 9.0	137.9± 9.2
Pore/a	0.3± 0.1	0.3± 0.1	0.3± 0.1
Filling fraction, FF (Diamond Minimum Surface)	0.4± 0.1	0.4± 0.1	0.4± 0.1

From the cross-sectional SEM images, we also estimate the domain sizes at the base and top

of the scale, see Table S2 in Supporting Information. In general, we observe that all three

weevils have scales thickness of 2-3 μm. In LPS, most domains range between 1.5 to 2.5 μm

in width (65 of the 67 domains investigated). In BPS, the width of the domain ranges between

2.5 and 3.5 μm (77 out of 79 domains investigated), while HPS has more varied domain

widths that range from 1.5 to 3.5 μm (60 domains observed). Additionally, we observe that:

(i) LPS has a smaller average domain size than BPS and HPS, and possesses many domains connecting both the top and the base of the scale; (ii) at the edges of the scale, domains that connect the top and the base of the scale can be observed while this is not the case at the centre of the scale.

2.3. FDTD simulation and visual color appearance

To correlate the orientation of the domains with the macroscopic optical response, we compute FDTD reflection spectra for the most abundant domains in each weevil, using the measured domain sizes, see Supporting Information Figure S4 A-C. The calculated spectra considering the effects of the domain width, domain thickness, the boundary conditions and presence of disorder are provided in Figure S5, and a complete discussion on how these parameters affect the optical response is also reported Supporting Information. This characterization allows us to assign each reflected color to a specific domain orientation identified *via* SEM. By comparing the histogram of colors obtained by RGB image analysis in **Figure 4** A, D, G (see Experimental Section) with the histogram of the domain orientations multiplied by the average lateral size of the domains in Figure 4 B, E, H, we show that the macroscopic color of each weevil is the sum of the contribution of individual domains, and that the distribution of orientations is the determining factor in the different color appearances of the three weevils. To facilitate the reader to visualise the correlation between the orientation of the domains with the macroscopic optical response, we plot the area covered by each oriented domain in three weevils on a stereographic projection as Figure 4 C, F, I as the insets in (Figure 4 in [40]).

In the projections, each marker corresponds to a specific domain orientation of the photonic structure inside the scale. The size of the markers is proportional to the area covered by the domain, and the color of the markers is chosen accordingly to the reflected color by the domains.

If we define a spherical coordinate system where the normal of crystal plane (100) as the zenith direction, (with φ defining the azimuthal angle, and θ defining the polar angle, see Supporting Information Figure S7 and Figure 3A), we observe different features of the angular relationships of preferred domain orientations in three weevils. The preferred domains orientations in LPS are along φ= 0°- 45°. In BPS, most of the domains are along φ=45° and 26.6° for which the reflected colors are red-shifted and domain coverage decreases from φ=26.6° to 0°. Preferred domain orientations in HPS are comparatively more evenly distributed. (See also Supporting Information "Domain orientations and domain color distributions" section, Figure S4 D-F and Table S3 for detail discussion).

We believe that the color-changing strategy of the hybrid weevil is interesting to design appearance with photonic materials because it relies on two main features that have high, but currently underexploited, potential: the combined use of an asymmetrical hierarchical structure and the optimization of size and distribution of domain with different orientation.

First, the photonic structure is confined into an asymmetrical scale that has a lateral size much larger than the thickness. Such a hierarchical feature allows minimizing the amount of material necessary to produce the desired coloration. In contrast, artificial hierarchical photonic structures propose so far usually consist of spherical structures, [41] where a significant fraction of the photonic crystal does not contribute to the optical response.

Second, the ability of the HPS to fine-tune color by optimization of domain size and distribution or the photonic crystal orientation, without a change of lattice constant. Such strategy is general and can be extended not only to bi-continuous types of photonic crystals but to any 3D and 2D ones. In contrast, the most used approach up to now to tune coloration in artificially photonic crystals systems is to change the lattice constant: requiring a change of the building blocks composing the photonic crystals, (nanosphere size in case of opal-like

structures made by colloidal self-assembly or polymer chain length in case of other photonic

crystals made of block-copolymers). [41-43]
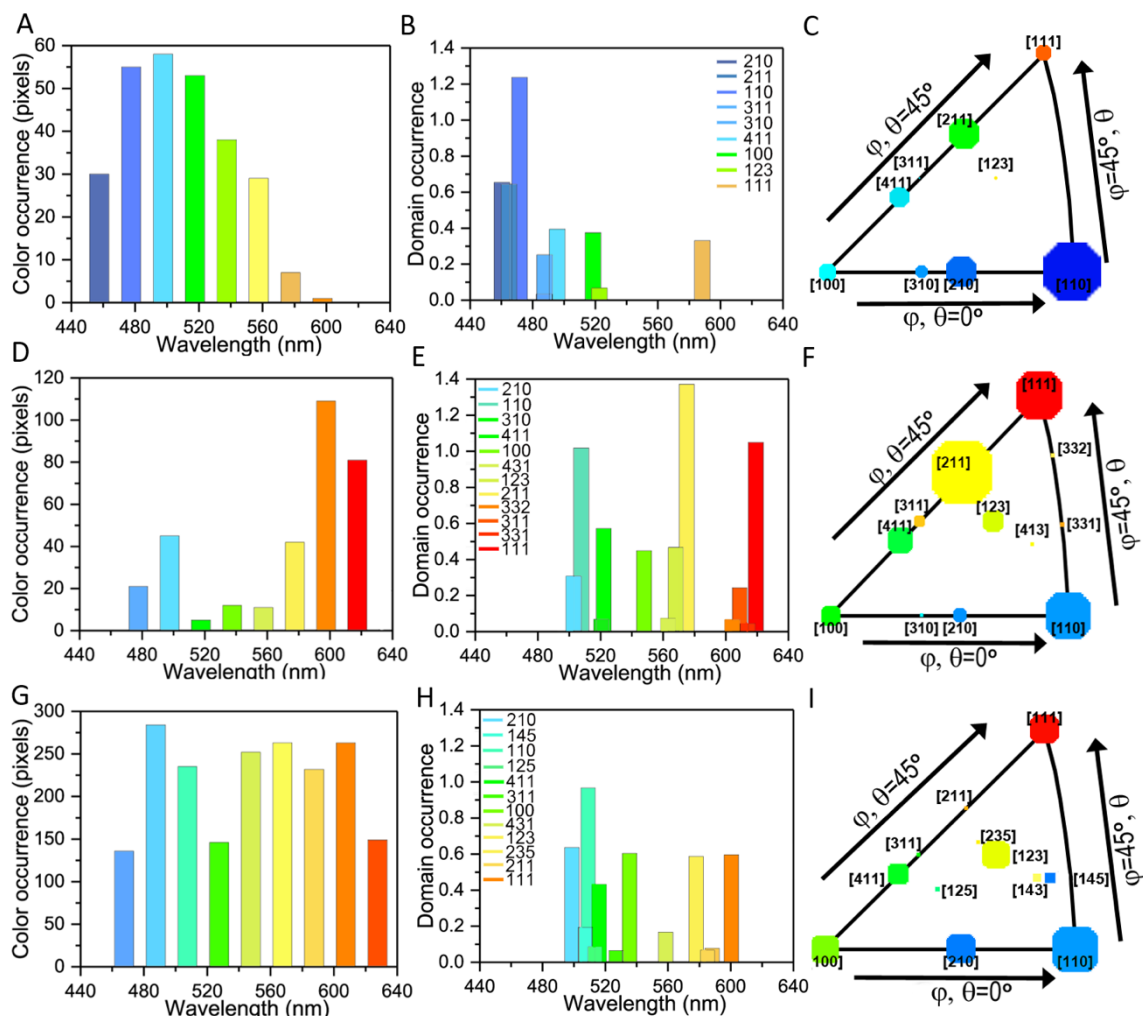
Figure 4 Comparison of color occurrence derived by RGB image analysis on optical

microscope images and domain occurrence derived by statistical analysis on SEM images of

(A- C) LPS, (D- F) BPS, (G- I) HPS. (**A, D, G**) show the distribution of color on the scales of

three weevils. The color histograms are obtained using image analysis on individual scales

and then averaging. In (**B, E, H**) we report the histogram of the area covered by each domain

orientation for three weevils. The domain occurrence is obtained by multiplying the number

of a domain with its average width and normalized on the average radius of the scale which is

38.08± 1.1 µm for LPS:,36.42± 0.5 µm for BPS, and 37.10± 6.3 µm for HPS. In (C, F, I) we

illustrate the preferred domain orientations in three weevils on stereographic projection with the marker size proportional to the domain occurrence and the marker color the same as the reflected color.

3. Conclusion

The possibility to captive-breed and hybridize different structurally colored *Pachyrhynchus* weevils allowed us to systematically investigate how photonic structures can be modified from ancestors to descendent only in one generation. By carefully studying the anatomy of the scales of the three weevils, we observed that the captive-bred hybrid *P. sarcitis* obtain green coloration by maintaining the lattice constant of its ancestors (BPS) and changing the domain size and orientations.

Interestingly, these observations remain valid irrespectively of the sex of the parents. Hybrid *P. sarcitis* weevils from blue and yellow parents are always green. To gather a full understanding of the heredity characters of this system will require genetic mapping of all animals. However, if we define the lattice constant of the photonic structure as a phenotypic trait, we can hypothesize that the genes of the BPS ancestor are dominant. By looking at the sequences of the different weevils, one would therefore expect to find similarities between the offspring and one parent generation, while similar occurrences are not expected to be found with the other parent. Additionally, if we consider the domain orientation as a possible phenotypic trait, we can conclude that the genetic variation in HPS seems to be additive as the domain orientation is about the average of those of the parents.

We speculate that changing orientation of domains to tune color might be more successful than an adjustment of the lattice constant if one consider that such nanostructures are obtained *via* self-assembly of an infolding lipid-bilayer membrane, followed by deposition of chitin

into the extra-cellular space. [7,17,21] In this hypothesis a change of lattice constant will, in fact, require a re-design of the biopolymers involved in the formation of these photonic structures, while changes in crystal domain orientations can be simply achieved by a change in surface properties in the scale interior membrane.

Moreover, a fast adaptation mechanism that can be obtained in one generation only might be of advantage under selection pressures from predation. This is further confirmed by the fact that the colored patches of *Pachyrhynchus* weevils are known to have aposematic functions [19,30] as their robust exoskeleton form a co-defense mechanism that efficiently reduces attack rate from local lizards. [19] In fact, several different genera of weevils [29,31] such as long-horned beetles (*Doliops* spp.) and crickets (*Scepastus pachyrhynchoides*) [29,31,38] occurring in the same geographical area display a similar bright pattern of colors. Finally, the possibility to study the hereditary character of structural colors in captive-bred species also allows, in future studies, to gain a better understanding of the development of such nanostructures.

By quantitatively correlating the measured optical response and anatomy of the hybrid *P. sarcitis* with the ones of its ancestors, we reveal how structural colors in *Pachyrhynchus* can be readily tuned in only one generation by adjusting the orientations of the photonic crystal domains in its scales. Monitoring how the structural colors traits can be passed to the first filial generation we speculate that poly-domains three dimensional photonic structures may represent a successful strategy for changing appearance in presence of strong selection pressure. Our result that the hybrid weevils have domain tilting and no change of the lattice constant provides an interesting inspiration for visual appearance design using self-assembly techniques for photonic materials. [41,43]

4. Experimental Section

Species Selections

Adults of *P. sarcitis* were collected from Babuyan (19°32' 58"N, 121°54' 40"E) and Lanyu (22°4'44.57"N, 121°33'15.25"E) Islands. These two populations have almost identical appearances, except coloration. Captive-breeding of Lanyu *P. sarcitis*, Babuyan *P. sarcitis* and hybrid *P. sarcitis* were conducted in the laboratory in National Taiwan University (Taipei, Taiwan). The detail of the breeding technique can be found in the paper. [37]

Optical microscopy and image analysis

Optical microscopy was performed using a Zeiss Axio Scope optical microscope in Köhler illumination equipped with a 50X SLWD objective (Nickon, NA=0.4) coupled to a spectrometer (Avantes HS2048) *via* an optical fiber (Thorlabs, FC-UV100-2-SR) (detected spot with diameter of a few μm). Spectra were normalized with a silver mirror (Thorlabs, PF10-03-P01). Scales were detached from the elytra and placed on glass slide. Spectra of different domains on each scale were measured. Domain color distribution was quantitatively analyzed by image-based RGB analysis on many single scales in each weevil with ImageJ Software (http://rsb.info.nih.gov/ij/). [39]

SEM sample preparation and image analysis

For the top view SEM images, scales were detached from the elytra and placed on a glass slide and plasma etched for 13 minutes to remove the outer shell of scales. The etched scales were transferred onto a SEM Stub and coated with 10 nm Pt for imaging. The SEM (Tescan MIRA3 FEG-SEM) used to observe the top view was operated at 3 kV with working distance of 5.2 mm and using an in-beam secondary electron detector.

For the cross-sectional imaging, the scales still attached to the elytra were directly embedded in Embed 812 resin (EMS, Hatfield, USA) and hardened overnight at 60 °C. After resin embedding, the scales were transversely cut (with a 35° diamond knife (Diatom, USA) equipped on a ultramicrotome Leica EM UC6 (Leica Microsystems, Germany) to expose their

WILEY-VCH

internal voids on the block face. Fresh resin was then applied again on the block face to fill

the inside of the scale. Once the resin set scales were cut again using the same setup. The

newly made block face was further treated with 2% osmium tetroxide aqueous solution to

enhance image contrast. The cross-sectional SEM observation was carried out with a field

emission SEM (Quanta-FEG 250, Thermo Fisher Scientific Inc., U.S.A.) operated at 7 kV and

using a concentric backscattering electron detector.

FDTD simulation

Three dimensional diamond models were constructed in MATLAB and 3D images were

obtained with Blender. Finite-difference time-domain (FDTD) calculations were performed

with the commercial software Lumerical. Different crystal orientations, characterized through

cross-sectional SEM images of scales, were oriented in the simulation box perpendicular to

the direction of light incidence. We modelled reflection properties of the chitin-air diamond

structures with experimentally determined refractive index n= 1.53 for chitin (measured *via*

index matching oils Cargille series A), and n = 1 for the air spaces. Diamond minimum

surface equation $f(X, Y, Z) = \cos(Z)\sin(X + Y) + \sin(Z)\cos(X - Y)$ [9] was used for

model construction, where $X = \frac{2\pi x}{a}, Y = \frac{2\pi y}{a}, Z = \frac{2\pi z}{a}$ with a the lattice constant,

and x, y and z the coordinates. To match the experimental measurement conditions, the

simulation models were constructed with measured domain sizes, boundary conditions were

set to perfectly matched-layer boundaries (PML) in x, y, z, and light source was set to

Gaussian distributed from 300-800 nm with numerical aperture (NA)=0.4. One simulation run

of these setups for one orientation in one weevil required a memory of approximately 30-60

GB and simulation time 6- 10 ns for 20- 36 calculation hours. The solution of domains with

bigger size require longer simulation time to converge. We have compared the FDTD results

with different boundary conditions: PML with different domain sizes and periodic boundary

conditions (Figure S5). FWHM and reflectance were also calculated considering effect of

numerical aperture and disorder. To correlate the color with the different orientations in the

three weevils, the simulation boundary conditions were set to be periodical for x and y

dimensions. The z direction was set to be PML to take into account the measured limited

thickness. This setting enables us to simulate a much smaller model in x, y dimension by

constructing a minimum repeated unit cell, so to save computation resources that for one

simulation run required a memory of approximately 0.5-0.8 GB, and shorter simulation time

of 3 ns for deriving convergent solutions in 0.5-1.5 calculation hours. Even though in this

setup, we lost the precision in domain width and assumed a plane wave light source (NA=0).

Supporting Information
Supporting Information is available from the Wiley Online Library or from the author.

Conflict of Interest
The authors declare no conflict of interest.

Author Contributions
Y.C., O.D.O, H.Y.T. and S.V. designed research; H.Y.T. captive-bred and hybridized Pachyrhynchus weevils; Y.C., Y.O., O.D.O. processed SEM data; Y.O. embedded, fixed and microtomed the samples for SEM imaging. Y.C. , O.D.O. measured domain spectra; Y.C. , O.D.O., S.V. performed and analyzed optical/SEM data; Y.C., O.D.O. conducted MPB and FDTD simulation; G.J. conducted semi-analytical analysis for disorder; Y.C. and H.Y.T. organized crystal structures of Entiminae subfamily and H.Y.T. analyzed the data for discussing biofunctions of structural color and phylogeny of Pachyrhynchus weevils; Y.C., Y.O., O.D.O., G.J., H.Y.T. and S.V. discussed results and commented on the manuscript. Y.C., H.Y.T. and S.V. wrote the paper.

Received: ((will be filled in by the editorial staff))
Revised: ((will be filled in by the editorial staff))
Published online: ((will be filled in by the editorial staff))

References

[1]   S.Kinoshita, *Structural Colors in the Realm of Nature*, World Scientific, **2008**.

[2]   S.Vignolini, N.Bruns, *Adv. Mater.* **2018**, *30*, 1801687.

[3]   V. E.Johansen, O. D.Onelli, L. M.Steiner, S.Vignolini, Photonics in Nature: From Order to Disorder. in *Funct. Surfaces Biol. III Divers. Phys. Phenom.*, Springer International Publishing, Cham, **2017**, pp. 53–89.

[4]   V. E.Johansen, L.Catón, R.Hamidjaja, E.Oosterink, B. D.Wilts, T. S.Rasmussen, M. M.Sherlock, C. J.Ingham, S.Vignolini, *Proc. Natl. Acad. Sci.* **2018**, *115*, 2652.

[5]   S.Vignolini, P. J.Rudall, A.V.Rowland, A.Reed, E.Moyroud, R. B.Faden, J. J.Baumberg, B. J.Glover, U.Steiner, *Proc. Natl. Acad. Sci.* **2012**, *109*, 15712.

[6]   K. R.Thomas, M.Kolle, H. M.Whitney, B. J.Glover, U.Steiner, *J. R. Soc. Interface* **2010**, *7*, 1699.

[7]   H.Ghiradella, *J. Morphol.* **1989**, *202*, 69.

[8]   R. W.Corkery, E. C.Tyrode, *Interface Focus* **2017**, *7*, 20160154.

[9]   K.Michielsen, D. G.Stavenga, *J. R. Soc. Interface* **2008**, *5*, 85.

[10]   M. E.McNamara, V.Saranathan, E. R.Locatelli, H.Noh, D. E. G.Briggs, P. J.Orr, H.Cao, *J. R. Soc. Interface* **2014**, *11*, 20140736.

[11]   R.Ebihara, H.Hashimoto, J.Kano, T.Fujii, S.Yoshioka, *J. R. Soc. Interface* **2018**, *15*, 20180360.

[12]   M. H.Bartl, J. W.Galusha, L. R.Richey, J. S.Gardner, J. N.Cha, *Phys. Rev. E - Stat. Nonlinear, Soft Matter Phys.* **2008**, *77*, 050904.

[13]   D.V.Nance, *Interim report*, **2013**.

[14]   M.Srinivasarao, *Chem. Rev.* **1999**, *99*, 1935.

[15]   H.Yin, B.Dong, X.Liu, T.Zhan, L.Shi, J.Zi, E.Yablonovitch, *Proc. Natl. Acad. Sci.* **2012**, *109*, 10798.

[16]   R. O.Prum, R. H.Torres, *J. Exp. Biol.* **2004**, *207*, 2409.

[17]   V.Saranathan, C. O.Osuji, S. G. J.Mochrie, H.Noh, S.Narayanan, A.Sandy, E. R.Dufresne, R. O.Prum, *Proc. Natl. Acad. Sci.* **2010**, *107*, 11676.

[18]   J. A.Endler, *Philos. Trans. - R. Soc. London, B* **1993**, *340*, 215.

[19]   H. Y.Tseng, C. P.Lin, J. Y.Hsu, D. A.Pike, W. S.Huang, *PLoS One* **2014**, *9*, e91777.

[20]   A. E.Seago, P.Brady, J. P.Vigneron, T. D.Schultz, *J. R. Soc. Interface* **2009**, *6*, S165.

[21]   B. D.Wilts, B. A.Zubiri, M. A.Klatt, B.Butz, M. G.Fischer, S. T.Kelly, E.Spiecker, U.Steiner, G. E.Schröder-Turk, *Sci. Adv.* **2017**, *3*, e1603119.

[22]   B. D.Wilts, V.Saranathan, *Small* **2018**, *14*, 1870212.

[23]   J. W.Galusha, L. R.Richey, M. R.Jorgensen, J. S.Gardner, M. H.Bartl, *J. Mater. Chem.* **2010**, *20*, 1277.

[24]   A. E.Seago, R.Oberprieler, V. K.Saranathan, *Integr. Comp. Biol.* **2019**.

[25]   B. D.Wilts, K.Michielsen, H.DeRaedt, D. G.Stavenga, *J. R. Soc. Interface* **2012**, *9*, 1609.

[26]   B. D.Wilts, K.Michielsen, J.Kuipers, H.De Raedt, D. G.Stavenga, *Proc. R. Soc. B Biol. Sci.* **2012**, *279*, 2524.

[27]   V.Saranathan, A. E.Seago, A.Sandy, S.Narayanan, S. G. J.Mochrie, E. R.Dufresne, H.Cao, C. O.Osuji, R. O.Prum, *Nano Lett.* **2015**, *15*, 3735.

[28]   R. K.Nagi, D. E.Montanari, M. H.Bartl, *Bioinspiration and Biomimetics* **2018**, *13*, 035003.

[29]   W.Schultze, *Philipp. J. Sci.* **1923**, *23*, 609.

[30]   C. Y.Lee, S. P.Yo, R. W.Clark, J. Y.Hsu, C. P.Liao, H. Y.Tseng, W. S.Huang, *J. Zool.* **2018**, *306*, 36.

[31]   Y.Hiraku, *Gekkan-Mushi* **2017**, *553*, 22.

[32]   A.Rukmane, *Acta Biologica Universitatis Daugavpiliensis.* **2017***, 17*, 85.

[33]   Y. T.Chen, H. Y.Tseng, M. L.Jeng, Y. C.Su, W. S.Huang, C. P.Lin, *Syst. Entomol.* **2017**, *42*, 796.

[34]   A. R.Parker, V. L.Welch, D.Driver, N.Martini, *Nature* **2003**, *426*, 786.

[35]   V.Welch, V.Lousse, O.Deparis, A.Parker, J. P.Vigneron, *Phys. Rev. E - Stat. Nonlinear, Soft Matter Phys.* **2007**, *75*, 041919.

[36]   V. L.Welch, J. P.Vigneron, *Opt. Quantum Electron.* **2007**, *39*, 295.

[37]   L. C.Huang, W. S.Huang, C. P.Lin, O. M.Nuñeza, H. Y.Tseng, H. C.Tang, *J. Asia. Pac. Entomol.* **2018**, *21*, 1233.

[38]   A.Barševskis, N.Savenkov, *Balt. J. Coleopterol.* **2013**, *13*, 91.

[39]   J.Schindelin, I.Arganda-Carreras, E.Frise, V.Kaynig, M.Longair, T.Pietzsch, S.Preibisch, C.Rueden, S.Saalfeld, B.Schmid, J.-Y.Tinevez, D. J.White, V.Hartenstein, K.Eliceiri, P.Tomancak, A.Cardona, *Nat. Methods* **2012**, *9*, 676.

[40] B.Winter, B.Butz, C.Dieker, G. E.Schröder-Turk, K.Mecke, E.Spiecker, *Proc. Natl. Acad. Sci.* **2015**, 112, 12911.

[41]   E. S. A.Goerlitzer, R. N.Klupp Taylor, N.Vogel, *Adv. Mater.* **2018**, 30, 1706654.

[42]   B. D.Wilts, P. L.Clode, N. H.Patel, G. E.Schröder-Turk, *MRS Bull.* **2019**, *44*, 106.

[43] M.Stefik, S.Guldin, S.Vignolini, U.Wiesner, U.Steiner, *Chem. Soc. Rev.* **2015**, *44*, 5076.

Table of contents

Hereditary character of photonics structure in *Pachyrhynchus sarcitis* weevils: color changes *via* one generation hybridization

Lung-Chun Huang, Yin Chang, Hui-Yun Tseng*, Silvia Vignolini*

Pachyrhynchus sarcitis from two different islands have evolved yellow (male) and blue scales (female) by each tuning the lattice constant of photonic crystals within their scales. Their first generation surprisingly possesses a mixing color of green which is independent of the sex of parents. Unexpectedly, the mixing color is not from an intermediate crystal structure but a different distribution of preferred crystal orientations.